Published in final edited form as:
Neurobiol Dis. 2008 April ; 30(1): 94–102. doi:10.1016/j.nbd.2007.12.005.

LRP promotes endocytosis and degradation, but not transcytosis, of the amyloid-β peptide in a blood-brain barrier *in vitro* model

Babak Nazer[1,2], **Soyon Hong**[1], and **Dennis J. Selkoe**[1]

1*Center for Neurologic Diseases, Brigham and Women's Hospital and Harvard Medical School, Boston, MA 02115, USA*

2*Howard Hughes Medical Institute, Chevy Chase, MD 20815, USA*

Abstract

The pathogenesis of Alzheimer's disease is characterized by aggregation of the amyloid-β protein (Aβ) into neurotoxic plaques. Recent *in vivo* studies have suggested the non-proteolytic clearance of Aβ via receptor-mediated transport across the blood-brain barrier (BBB). The aim of this study was to investigate the role of p-glycoprotein (Pgp) and the low-density lipoprotein receptor-related protein (LRP) in Aβ efflux across the BBB. We developed an *in vitro* BBB-like model using Madin Darby Canine Kidney (MDCK) cells seeded on filters separating apical (blood) and basolateral (brain) compartments. MDCK cells were stably transfected with Pgp or mLRP4, an LRP mini-receptor. When compared to empty vector-transfected cells, MDCK-Pgp cells did not transcytose radiolabeled Aβ in the basolateral-to-apical direction. MDCK-mLRP4 cells were found to endocytose and degrade, but not to trasncytose intact radiolabeled Aβ. These results implicate LRP as a mediator of Aβ degradation, but indicate that overexpression of LRP or Pgp alone is insufficient for non-proteolytic transcytosis of intact Aβ.

Keywords

Alzheimer's disease; Amyloid-β protein; Blood-brain barrier; Low-density lipoprotein receptor-related protein; MDCK cells; P-glycoprotein

Introduction

Alzheimer's disease (AD) is the most common cause of dementia, with over 30 million people are affected world-wide. A key neuropathological lesion in AD, the neuritic plaque, consists of extracellular deposits of the amyloid-β protein (Aβ). Accumulation of Aβ is believed to initiate AD when there is an imbalance between its production and clearance, leading to its aggregation into oligomers and neuritic plaques (Hardy and Selkoe, 2002).

Research into therapeutic avenues to lower cerebral Aβ levels has largely centered on decreasing its production by inhibiting the proteases that generate Aβ (Selkoe and Schenk, 2003), increasing its clearance through immunotherapy (Weiner and Frenkel, 2006), or

Corresponding Author: DJ Selkoe, Harvard Institutes of Medicine Room 730, 77 Avenue Louis Pasteur, Boston, MA 02115, USA, Telephone: 617-525-5200, Fax: 617-525-5252, E-mail address: dselkoe@rics.bwh.harvard.edu.

promoting its degradation by proteases such as insulin-degrading enzyme and neprilysin (Tanzi et al., 2004). In addition, non-proteolytic clearance by receptor-mediated transport of Aβ out of the CNS has been investigated as another potential mechanism for decreasing cerebral Aβ load. Two pathways for Aβ transport out of the CNS exist: bulk flow (Silverberg et al., 2003) of interstitial fluid (ISF) into the blood via the cerebrospinal fluid (CSF), and transcytosis of Aβ across the blood-brain barrier (BBB). It has been reported that CSF-mediated bulk flow accounts for no more than 10–15% of non-proteolytic transport of Aβ out of the CNS *in vivo* (Shibata et al., 2000), leaving the BBB as the main route of efflux. The BBB is distinct from other cell barriers by its increased tight junction density, lower rates of non-selective pinocytosis, lack of fenestrations, and unique cell surface receptor expression profile (Rubin and Staddon, 1999). A few such receptors for Aβ transport have been described (Zlokovic, 2004).

Low-density lipoprotein receptor-related protein (LRP) is a ~600 kDa multi-ligand cell surface receptor that is highly expressed in brain and contains four extracellular ligand-binding domains (designated I–IV). Over 30 different ligands for LRP have been reported and include the classes: lipoproteins, coagulation factors, growth factors, extracellular matrix proteins, chaperones, and bacterial/viral proteins. The majority of LRP ligands bind to domains II and IV with equal affinity (Cam and Bu, 2006). Investigation into LRP's role in AD was stimulated by genetic evidence linking the *LRP* gene to late-onset AD (Kang et al., 1997). Zlokovic and colleagues first reported LRP's effects on Aβ efflux, showing that the *in vivo* clearance of radiolabeled Aβ peptides injected into the brains of mice was inhibited by co-injection with the endogenous inhibitor receptor-associated peptide (RAP) and by an anti-LRP antibody (Shibata et al., 2000). *In vivo* studies of LRP's potential for effluxing Aβ are promising, but they do not identify the biochemical mechanism of the apparent transcytosis of intact Aβ across the endothelial cells of the BBB. Moreover, as a member of the LDL receptor family, LRP is primarily an endocytic receptor and is not generally known to transcytose its ligands, most of which are degraded in lysosomes after endocytosis (Krieger and Herz, 1994).

P-glycoprotein (Pgp) is a 170 kDa single-transmembrane protein known for its role in resistance to chemotherapeutic drugs (Sharom, 1997). *In vivo* work has shown that PGP-null mice clear microinjected [^{125}I]Aβ out of the CNS at half the rate of wt mice and that Aβ increases within brain ISF after treatment with a Pgp inhibitor (Cirrito et al., 2005). As with LRP, the mechanism of Pgp-mediated Aβ efflux is unknown and has not been studied in controlled culture models of the BBB. All known substrates of Pgp are small molecules and cytosolic, whereas Aβ is a peptide and is not known to exist in the cytosol. While *in vivo* work has thus generated much excitement with regard to the potential of LRP and Pgp to efflux cortical Aβ, elucidating the molecular mechanisms of these effects through well-controlled *in vitro* models should help to promote rational therapeutic design.

Madin Darby canine kidney (MDCK) cells are routinely used as a model of polarized protein sorting and trafficking (Irvine et al., 1999), and have been used previously to investigate polarization of amyloid-β precursor protein (APP) and its proteolytic products, Aβ and the secreted ectodomain, APPs (Haass et al., 1994). An *in vitro* model of a polarized epithelial barrier having tight intercellular junctions can be created by plating MDCK cells onto a porous polycarbonate filter, separating apical (AP) and basolateral (BL) compartments of medium, representing the brain and blood compartments, respectively, of a BBB-like barrier. MDCK monolayers plated in this manner have been used to investigate transcytosis of cell-surface proteins (Brandli et al., 1990), as well as antibody-antigen complexes (Hunziker and Mellman, 1989). MDCK monolayers have been used to simulate transport across the BBB (Garberg et al., 2005; Gumbleton and Audus, 2001). Despite its epithelial origin, this polarized, immortalized and impermeable system provides a manipulable model for investigating the effects of Pgp and LRP on Aβ BBB transport.

Materials and Methods

Cell Culture

MDCK wt cells (ATCC, Manassas, VA) were grown in DMEM with 10% FBS, 2 mM L-glutamine, 100 U/ml penicillin, 100 μg/ml streptomycin and 20 mM HEPES buffer. MDCK cells stably transfected with Pgp (MDCK-Pgp) or empty vector (MDCK-Parental) were the generous gift of Dr. P.Borst (Bakos et al., 1998). MDCK-Pgp cells were grown in the same media as MDCK wt cells and replaced with frozen stocks after one month of passage. MDCK cells stably transfected with mLRP4 (MDCK-mLRP4), an LRP-minireceptor which contains the native C-terminus and transmembrane domain, a N-terminal hemagglutinin (HA) tag, but only one (IV) of its four ligand-binding domains (Obermoeller-McCormick et al., 2001), were the generous gift of Dr. M. Marzolo (Marzolo et al., 2003). MDCK-mLRP4 cells were grown in the same media as MDCK cells, with the addition of 200 μg/ml G418. An immortalized human brain endothelial cell line, HCMEC/D3 (Weksler et al., 2005), was generously provided by Dr. B. Weksler, and grown in EGM-2 endothelial cell media (Lonza Group, Basel, Switzerland) on dishes coated with 50 μg/ml rat tail collagen I (BD Biosciences, Franklin Lakes, NJ).

In Vitro Transwell MDCK Model

MDCK cells were plated onto 6.5 mm diameter Transwell filters (Corning Life Sciences, Acton, MA) with 0.4 μm pores at a seeding density of 1×10^5 cells per filter. Media was changed daily, with 100 μl in the apical (AP) compartment and 600 μl in the basolateral (BL) compartment. Trans-epithelial electrical resistance (TEER) was measured using an EVOM epithelial volt-ohmmeter with STX2 electrodes (World Precision Instruments, Sarasota, FL). Background resistance across a non-seeded filter was subtracted from the TEER measurements. Models were used for Aβ transport experiments on day 5. [^{125}I]Aβ_{40}, [^{14}C] Inulin or [^{3}H]Verapamil (GE Healthcare Bio-sciences, Piscataway, NJ) were added to the media in the BL side of the Transwell filters at concentrations of 1 nM, 0.5 μCi/ml and 1 μCi/ml, respectively. For inhibition of Pgp, 25 μg/ml RU-486 (Biomol International, Plymouth Meeting, PA) was added to AP and BL media immediately before transport experiments. At each timepoint, 10 μl samples of AP and BL medias were counted on a Cobra II Auto-Gamma scintillation counter (Packard Biosciences, Shelton, CT) for ^{125}I, or on a Beckman-Coulter LS6500 scintillation counter (Beckman-Coulter, Fullerton, CA) for ^{14}C or ^{3}H. To determine the amount of intact radiolabeled peptide, 50μl of 15% trichloroacetic acid was added to a 50 μl sample of media and centrifuged at 10,000 × g for 10 minutes. Supernatant (degraded peptide) and pellet (intact peptide) were counted separately for [^{125}I].

Transport of each compound across the monolayers was calculated as the percentage of the total counts per minute that were detected in the AP compartment. For Aβ transport, to control for paracellular leak in each Transwell monolayer, both [^{14}C]inulin and [^{125}I]Aβ were added to BL compartments, and an Aβ clearance quotient (Aβ CQ) was calculated as below:

$$A\beta CQ = \frac{[^{125}I]_{AP}/([^{125}I]_{AP}+[^{125}I]_{BL})}{[^{14}C]_{AP}/([^{14}C]_{AP}+[^{14}C]_{BL})}$$

Polarized Cell Surface Biotinylation and Gel Electrophoresis

MDCK wt or MDCK-mLRP4 cells were plated onto 24mm diameter Transwell filters with 0.4 μm pores at a seeding density of 1×10^5 cells per filter and grown for five days with 1.5 ml AP and 2.5 ml BL media. Monolayers were washed on both sides with cold PBS with Ca^{2+} and Mg^{2+} (PBS^{++}) four times. EZ-link Sulfo-NHS-SS-biotin (Pierce Biotechnology, Rockford, IL) was dissolved to 1 mg/ml in cold HBSS and 1 ml was added to either AP or BL compartments. One ml PBS^{++} was added to the non-biotinylated side. Monolayers were rocked

for 1 hr at 4°C, and 50 µl quenching solution (Pierce) was added to the biotinylated side. Cells were scraped and lysed in 1% NP40 lysis buffer with protease inhibitors. After normalizing for total protein concentrations using a bicinchoninic assay (Pierce), the cell lysate was precipitated with 1 ml immobilized NeutrAvidin gel (Pierce) per 3 mg total protein overnight with mixing at 4°C. Immobilized Neutravidin gel was centrifuged at 2500 × g for 2 minutes. Biotinylated proteins were eluted with SDS-PAGE sample buffer with 50 mM DTT.

Samples were electrophoresed on an 8% Tris-Glycine gel (Invitrogen, Carlsbad, CA) and immunoblotted with 3F10 rat monoclonal anti-HA antibody (Roche, Basel, Switzerland) for detection of mLRP2, or C219 monoclonal mouse anti-Pgp antibody (ID Labs, London, Ontario).

Detection and immunoprecipitation of LRP in Cell Lysates

For detection of LRP, HCMEC/D3, HUVEC, MDCK wt and MDCK-mLRP4 cells were cultured to 80% confluency on 150-mm plates. Cells were washed three times with cold PBS with Ca^{2+} and Mg^{2+}, and were lysed in 300 µl of 1% Triton X-100 (Sigma) lysis buffer with 1 mM PMSF and protease inhibitors (Roche). Total protein was quantified using bicinchoninic acid protein assay (Pierce). 20 µg of cell lysates were boiled at 100°C for 5 minutes in a 4X lithium dodecyl sulfate (LDS) sample buffer containing 50 mM DTT, then were electrophoresed at 200 V on a 9-well 4–12% Bis-Tris gel for 35 minutes in a MES SDS running buffer (Invitrogen). Proteins were transferred onto 0.2 µm nitrocellulose and detected by western blotting using the Li-Cor Odyssey Infrared Imaging System after probing for LRP with MMMM, a rabbit polyclonal anti-LRP tail antibody (antibody kindly provided by Dr. G. Bu).

For immunoprecipitation of LRP, lysates of HCMEC/D3 cells from 150-mm plates were prepared in 1 ml non-denaturing lysis buffer (20 mM Tris HCl pH 8 containing 137 mM NaCl, 10% glycerol, 1% Nonidet P-40 (NP-40) and 2 mM EDTA) with protease inhibitors (Roche). 300 µl of lysate was pre-cleared with 20 µl protein A-coupled sepharose (PAS) beads (Sigma) and 20 µl protein G-coupled agarose (PGA) beads (Roche) for 1 hour under rotary agitation at 4°C. Non-specifically bound proteins to beads were spun out, and supernatants were incubated with 5A6, an anti-LRP light-chain mouse monoclonal antibody (Calbiochem) and 15 µl each of PAS and PGA beads at 4°C under rotary agitation overnight. Beads were then spun out and washed in lysis buffer three times. After the final wash, pellet was boiled at 100° C for 5 minutes in 2X LDS sample buffer containing 50 mM DTT (Invitrogen) to denature and reduce the protein, and to separate it from the beads. The samples were centrifuged, and supernatants were electrophoresed to detect LRP via WB as described above.

FACS-based Aβ Endocytosis Assay

HCMEC/D3, MDCK wt or MDCK-mLRP4 cells were plated onto 6-well dishes at a seeding density of 1×10^5 cells per well and allowed to grow overnight. 500 nM RAP (Oxford Biomedical Research, Oxford, MI) was added to inhibit LRP activity in some wells. At this concentration, RAP is most selective for inhibition of LRP, while minimizing cross-inhibition of receptors in the same family, VLDL-R and LDL-R (Holtzman, personal communication). 100 nM fluorescently-labeled HiLyte Fluor 555-$A\beta_{1-40}$ or HiLyte Fluor 488-$A\beta_{1-42}$ (AnaSpec, San Jose, CA) were added at various timepoints, and cells were washed twice with PBS and then removed from the plate using 0.25% trypsin/EDTA solution. Cells were centrifuged at 800 × g for 5 min, and resuspended in 100 µl PBS with 10% BSA. Five µl 7-amino-actinomycin D (7-AAD; BD Biosciences) was added for 10 min prior to analysis to control for cell viability. 1×10^5 cells from each sample were analyzed for fluorescence on a BD FACSCalibur machine (BD Biosciences). Unstained cells without any exposure to fluorescently-labeled Aβ were used

as a control for background fluorescence of, and Aβ uptake was quantified as the percentage of non-7-AAD-containing cells in each sample above the background level of fluorescence.

Radioactivity-based Aβ Endocytosis Assay

HCMEC/D3, MDCK wt or MDCK-mLRP4 cells were plated as in the FACS-based assay above. 1 nM [^{125}I]Aβ was added to each well at various timepoints, and cells were removed as in the FACS-based assay. Cell pellets were lysed in 100 μl of 1% NP40 lysis buffer with protease inhibitors. 10 μl samples of the lysate were analyzed for [^{125}I] counts, and 50 μl was precipitated with 50 μl TCA as described above.

Statistical Analysis

Data was analyzed using a one-way ANOVA with Tukey's *post hoc* comparison or a two-way ANOVA with Bonferroni *post hoc* comparison, where appropriate. Calculated comparisons of $p < 0.05$ were considered significant.

Results

Assessment of Transwell MDCK Model of the BBB

In order to simulate the integrity of the BBB, an *in vitro* model must demonstrate adequate tight junction formation as well as impermeability to macromolecules. To assess the former, the trans-epithelial electrical resistance (TEER) of Transwell MDCK monolayers was measured daily after plating, reaching an average of 85.8 ± 0.60 Ω*cm^2 (mean ± SD; n=22) after 5 days (Fig. 1A). As with most *in vitro* BBB models, this value falls far short of recorded values for the *in vivo* BBB of 1870 ± 639 Ω*cm^2 (mean ± SD; n=40) (Crone and Olesen, 1982), but it is greater than achieved in most endothelial cell *in vitro* models (Garberg et al., 2005). TEER of MDCK cells transfected with Pgp or mLRP4 was not significantly different from that of MDCK wt cells (data not shown).

The inert polysaccharide, inulin (1.7 kDa) is routinely used as a control for paracellular leak in models of epithelial and endothelial barriers given its lack of active, receptor-mediated transport. [^{14}C]Inulin was added to the BL side of MDCK cell-seeded and non-seeded control Transwell filters, and radioactivity of media on both sides was counted at 2, 6, 12, 24 and 48 hr. At 48 hr, MDCK cell-seeded BBB models remained quite impermeable to inulin, with only 2.3% of [^{14}C]inulin counts crossing to the AP compartment compared to 50.3% that freely diffuses across non-seeded filters (Fig. 1B). To determine the ability of MDCK wt cells to transport Aβ, the same experiment was performed with [^{125}I]Aβ_{40}, with 2.7% crossing MDCK cell-seeded filters compared to 49.1% across non-seeded controls (Fig. 1B). The high TEER values and low [^{14}C]inulin permeability across MDCK wt cells indicates that MDCK Transwell monolayers provide a BBB-like model with low paracellular leak for the investigation of macromolecular transport. Furthermore, because permeability of MDCK wt monolayers to inulin and Aβ was similar, these cells represent a manipulable model in which transfection with LRP, Pgp, or other potential Aβ transporters can be shown to promote Aβ transport across the BBB, elucidating its mechanism.

MDCK-Pgp BBB Models

Expression of Pgp by MDCK-Pgp cells was verified by Western blotting. Pgp expression was significantly greater in the MDCK-Pgp cell line, although some expression was seen in the empty vector-transfected (MDCK-Parental) line (Fig. 2A). This was likely due to cross-reacting endogenous expression of canine ABC-family transporters including Pgp, as seen previously (Lalloo et al., 2004).

Verapamil, a known substrate for Pgp that is preferentially effluxed across the BBB by this transporter, was used to determine functional expression of Pgp in the cells. [^{3}H]Verapamil was added to the BL compartment of Transwell filters of MDCK-Pgp and MDCK-Parental monolayers. After 6 hr, 60.0% of [^{3}H]verapamil had been transported to the AP compartment of MDCK-Pgp monolayers, as compared with 47.4% for MDCK-Parental monolayers. When RU-486, a pharmacological inhibitor of Pgp, was added to MDCK-Pgp monolayers, the 6 hr transport was rescued to 45.3%, near that of MDCK-Parental control cells (Fig. 2B). These results indicate functional expression of Pgp in the MDCK-Pgp cell line. The high background level of [^{3}H]verapamil transport in MDCK-Parental cells and after RU-486 treatment of MDCK-Pgp cells is presumably due to passive paracellular and transcellular leak of the small molecule, as well as to activity of other endogenous ABC-family transporters, many of which are not inhibited by RU-486.

To determine the ability of Pgp to transcytose Aβ, 1 nm [^{125}I]Aβ was added to the BL compartment of MDCK-Pgp and MDCK-Parental control Transwell monolayers. After 48 hr, there was very little transport of [^{125}I] counts from the BL to AP compartment in both the MDCK-Pgp and MDCK-Parental monolayers (0.56% vs 0.47%, $p>0.05$) (Fig. 2C). There was also no significant difference in the Aβ clearance quotient (Fig. 2D), indicating that all of the apically-localized Aβ was due to paracellular leak and that upregulation of Pgp alone is insufficient to promote Aβ transcytosis across this *in vitro* BBB model.

MDCK – mLRP4 BBB Models

MDCK cells stably expressing the LRP minireceptor, mLRP4, or non-transfected controls (MDCK wt) were plated on Transwell filters. To determine expression and polarity of mLRP4, the AP and BL sides of the monolayers were biotinylated separately, and plasma membrane proteins were precipitated with neutravidin and analyzed by Western blotting. LRP and its minireceptors are known to be cleaved by furin to yield the mature, functional version of the receptor (Obermoeller-McCormick et al., 2001). Both immature and mature forms were expressed on the BL surface of our Transwell BBB model, but only the immature form was expressed on the AP surface (Fig. 3A).

To determine the ability of LRP to transcytose Aβ, 1 nm [^{125}I]Aβ was added to the BL compartment of MDCK-mLRP4 and MDCK wt Transwell monolayers. After 48 hr, 11.8% of total [^{125}I] counts in MDCK-mLRP4 Transwell monolayers were found in the AP compartment, compared to 4.0% in MDCK wt monolayers (Fig. 3B). The Aβ clearance quotient was significantly higher for MDCK-mLRP4 monolayers than for MDCK wt monolayers (Fig. 3C), indicating a selective transport of [^{125}I]Aβ. However, when AP and BL media were precipitated with TCA to quantify the intact Aβ peptide, we found that 81.9% of the [^{125}I]Aβ in the BL compartment of MDCK wt monolayers at 48 hr was still intact, whereas only 9.6% remained intact at 48 hr in the BL compartment of the MDCK-mLRP4 monolayers (Fig. 3D). In the AP compartments, virtually all of the [^{125}I] counts that reached this compartment represented degraded peptide in both the MDCK wt and MDCK-mLRP4 monolayers (Fig. 3E), suggesting that only fragments of Aβ efficiently cross the *in vitro* barrier from the BL to AP side. These findings suggest that the overexpression of LRP on the BL plasma membrane promotes Aβ degradation, but alone is insufficient to promote the transcytosis of the intact peptide, as would be required for non-proteolytic efflux of Aβ across the barrier.

LRP-Mediated Aβ Endocytosis and Degradation

The reported role of LRP for all studied ligands besides Aβ is to bind, endocytose and facilitate their degradation. In accord with these data, expressing mLRP4 on the BL plasma membrane in our MDCK monolayer resulted in no LRP-mediated transport of intact [^{125}I]Aβ, but rather

transport of [^{125}I]-bearing cleaved peptide fragments. To directly address this process, MDCK wt and MDCK-mLRP4 cells were grown in conventional cultures and exposed to 1 nM [^{125}I] Aβ. At 24 hr, the cells were washed to remove surface peptide, lysed and samples of the lysate counted for internalized [^{125}I]. We found that [^{125}I]Aβ uptake was markedly greater in MDCK-mLRP4 than MDCK wt cells (1543 vs 166 CPM; Fig. 4A). Samples of the lysate (Fig. 4B) were then precipitated with TCA to determine the percentage of intact Aβ. In MDCK-mLRP4 cultures, significantly more intracellular Aβ had been degraded by 24h compared with MDCK wt cultures (74.7 vs 7.1%) (Fig. 4B).

While the MDCK monolayer presents a polarized, impermeable and manipulable system for the investigation of LRP's effects on Aβ transcytosis, it is not of endothelial origin. To determine the effects of LRP on Aβ endocytosis and degradation in an endothelial cell culture, immortalized HCMEC/D3 cells, which are of human brain endothelial origin, were used in a similar experiment. First, we determined LRP expression in HCMEC/D3 cells, as well in the positive controls human umbilical vein endothelial cells (HUVEC) and MDCK-mLRP4 cells by western blotting with MMMM rabbit polyclonal anti-LRP light chain antibody. A faint 85 kDa band was seen in the HCMEC/D3 lane (Fig. 4C), consistent with expression of the LRP light chain. This expression was verified by immunoprecipitation of the LRP light chain with MMMM, and western blotting with 5AG, a mouse monoclonal anti-LRP light chain (Fig. 4D).

HCMEC/D3 cells were incubated with 1 nM [^{125}I]Aβ in the presence or absence of 500 nM RAP to inhibit endogenous LRP activity. [^{125}I]Aβ uptake (33 vs 737 CPM) (Fig. 4E) and degradation (2.3 vs 44.2%) (Fig. 4F) were decreased in the presence of RAP. As with primary endothelial cells and other immortalized endothelial lines, when these cells were seeded onto Transwell filters, they failed to achieve adequate TEER or inulin impermeability to allow investigation of Aβ transcytosis (data not shown).

Theoretically, a radiolabel could alter the physiologic function or activity of a peptide. To further confirm the ability of LRP to promote Aβ endocytosis by using a different label on the peptide, fluorescently-labeled Aβ was added to MDCK-mLRP4 and MDCK wt cells in culture at various time points, and the fluorescent cells that had endocytosed Aβ were counted using FACS. As with the radiolabeled Aβ, the uptake of HiLyte Fluor 555-$Aβ_{1–40}$ was time-dependent and significantly greater with MDCK-mLRP4 cells than with MDCK wt cells (42.7% vs 8.41% at 24 hr) (Fig. 5A). Addition of RAP significantly decreased Aβ uptake by MDCK-mLRP4 cells down to 29.5% at 24 hr (Fig. 5A). Similar results were obtained for uptake of fluorescently-labeled $Aβ_{42}$ (data not shown).

Finally, HCMEC/D3 cells were used in the same FACS-based Aβ uptake assay. Their $Aβ_{40}$ uptake was also time-dependent and significantly inhibited by RAP (Fig. 5B).

Discussion

As the Aβ hypothesis has gained increasing acceptance as the apparent mechanism of AD pathogenesis, investigation surrounding potential strategies to chronically decrease cortical Aβ levels has intensified. Of several such approaches, the non-proteolytic clearance of Aβ by efflux across the BBB is perhaps the least studied, and the biochemical basis for this phenomenon is unclear. The promising *in vivo* work identifying Pgp and LRP as potential Aβ efflux pumps needs to be followed up using controlled *in vitro* models to help elucidate the molecular basis for the apparent transport of Aβ across cell barriers by these proteins.

The MDCK *in vitro* model we principally used here, while of epithelial rather than endothelial origin, is a useful tool for the mechanistic investigation of potential Aβ transporters across tight monolayer barriers. These cells readily form monolayers that are polarized and impermeable to macromolecules—two properties that are vital to investigation of Aβ transcytosis, and that

have not been readily reproduced in many endothelial BBB models. Furthermore, MDCK cells can be transfected with Pgp, LRP minireceptors, or other gene products that may be implicated in the process of Aβ efflux across the BBB.

In our study, MDCK cells stably overexpressing Pgp did not exhibit any increased transport of [^{125}I]Aβ across their monolayers when compared with MDCK cells transfected with empty vector and cultured identically. Although they functionally expressed Pgp, as evidenced by the efficient efflux of [^{3}H]verapamil that was inhibited by RU-486, the upregulation of Pgp alone was not sufficient to promote Aβ transcytosis as has been suggested by *in vivo* experiments in which Pgp-null mice clear CNS-injected Aβ at a lower rate than did wt mice, and in which administration of a Pgp inhibitor increased Aβ levels in the brain ISF within hours (Cirrito et al., 2005). Because Pgp is a transporter whose ligands are almost exclusively small molecules (no peptide substrates of Pgp have been identified), it is not surprising that the pump itself is unable to transport a 4 kDa peptide such as Aβ. It is possible that Pgp functions in conjunction with another transporter or requires an as-yet-unidentified cofactor for Aβ transcytosis such that its inhibition or deletion *in vivo* inhibited Aβ clearance and increased cortical Aβ levels but its upregulation failed to promote Aβ efflux in our cellular model.

In our MDCK-mLRP4 model, LRP activity led to the uptake and degradation of [^{125}I]Aβ from the BL compartment, but not to transcytosis of the intact peptide in its intact form, as has been suggested by the results of *in vivo* experiments (Shibata et al., 2000). As with Pgp, the effects of LRP seen in our study are more congruent with its accepted biological mechanism—as an endocytic receptor that usually leads to degradation of its ligands. Any role it may have in transcytosing intact Aβ across the BBB, as in the case with Pgp, may require a co-transporter, or a downstream molecule. Nevertheless, our results clearly implicate LRP as a means of promoting Aβ degradation and help to explain the apparent relationship between down-regulation of LRP and progression of AD pathology in humans (Deane et al., 2004). Although it has been shown that complexes of Aβ and its binding partner α2-macroglobulin can be endocytosed by LRP (Kang et al., 2000), we demonstrate the ability of LRP to not only endocytose, but also lead to the degradation of the pathologic peptide.

There currently exists a disconnect between the accepted biological mechanisms of Pgp and LRP, with which our *in vitro* experiments are consistent, and the *in vivo* findings regarding LRP- and Pgp-mediated Aβ efflux across the BBB in rodents. More *in vitro* work on these two transporters and others that may serve as co-transporters in Aβ efflux may help to reconcile these differences. A compelling *in vitro* BBB model is invaluable to such efforts. While current endothelial monolayer systems need to be improved to create more impermeable and physiologic BBB models, the MDCK Transwell model described here is an impermeable, polarized and biochemically readily manipulable system for such invenstigations.

Acknowledgments

We would like to thank Drs. Piet Borst, Guojun Bu, María Paz Marzolo and Babette Weksler for their generous contribution of cell lines used in this study. We would also like to thank Drs. David Holtzman and Berislav Zlokovic for their advice regarding experimental design, and Drs. Joseph El Khoury and Danny Frenkel for their training on the methods used in this study. We would like to thank Matthew Hemming for his critical review of this manuscript. Babak Nazer is a Howard Hughes Medical Institute Research Training Fellow.

References

Bakos E, et al. Functional multidrug resistance protein (MRP1) lacking the N-terminal transmembrane domain. J Biol Chem 1998;273:32167–32175. [PubMed: 9822694]

Brandli AW, et al. Transcytosis in MDCK cells: identification of glycoproteins transported bidirectionally between both plasma membrane domains. J Cell Biol 1990;111:2909–2921. [PubMed: 2269660]

Cam JA, Bu G. Modulation of beta-amyloid precursor protein trafficking and processing by the low density lipoprotein receptor family. Mol Neurodegener 2006;1:8. [PubMed: 16930455]

Cirrito JR, et al. P-glycoprotein deficiency at the blood-brain barrier increases amyloid-beta deposition in an Alzheimer disease mouse model. J Clin Invest 2005;115:3285–3290. [PubMed: 16239972]

Crone C, Olesen SP. Electrical resistance of brain microvascular endothelium. Brain Res 1982;241:49–55. [PubMed: 6980688]

Deane R, et al. LRP/amyloid beta-peptide interaction mediates differential brain efflux of Abeta isoforms. Neuron 2004;43:333–344. [PubMed: 15294142]

Garberg P, et al. In vitro models for the blood-brain barrier. Toxicol In Vitro 2005;19:299–334. [PubMed: 15713540]

Gumbleton M, Audus KL. Progress and limitations in the use of in vitro cell cultures to serve as a permeability screen for the blood-brain barrier. J Pharm Sci 2001;90:1681–1698. [PubMed: 11745727]

Haass C, et al. Polarized secretion of beta-amyloid precursor protein and amyloid beta-peptide in MDCK cells. Proc Natl Acad Sci U S A 1994;91:1564–1568. [PubMed: 8108445]

Hardy J, Selkoe DJ. The amyloid hypothesis of Alzheimer's disease: progress and problems on the road to therapeutics. Science 2002;297:353–356. [PubMed: 12130773]

Hunziker W, Mellman I. Expression of macrophage-lymphocyte Fc receptors in Madin-Darby canine kidney cells: polarity and transcytosis differ for isoforms with or without coated pit localization domains. J Cell Biol 1989;109:3291–3302. [PubMed: 2574723]

Irvine JD, et al. MDCK (Madin-Darby canine kidney) cells: A tool for membrane permeability screening. J Pharm Sci 1999;88:28–33. [PubMed: 9874698]

Kang DE, et al. Modulation of amyloid beta-protein clearance and Alzheimer's disease susceptibility by the LDL receptor-related protein pathway. J Clin Invest 2000;106:1159–1166. [PubMed: 11067868]

Kang DE, et al. Genetic association of the low-density lipoprotein receptor-related protein gene (LRP), an apolipoprotein E receptor, with late-onset Alzheimer's disease. Neurology 1997;49:56–61. [PubMed: 9222170]

Krieger M, Herz J. Structures and functions of multiligand lipoprotein receptors: macrophage scavenger receptors and LDL receptor-related protein (LRP). Annu Rev Biochem 1994;63:601–637. [PubMed: 7979249]

Lalloo AK, et al. Membrane transport of camptothecin: facilitation by human P-glycoprotein(ABCB1) and multidrug resistance protein 2 (ABCC2). BMC Med 2004;2:16. [PubMed: 15125776]

Marzolo MP, et al. Differential distribution of low-density lipoprotein-receptor-related protein (LRP) and megalin in polarized epithelial cells is determined by their cytoplasmic domains. Traffic 2003;4:273–288. [PubMed: 12694565]

Obermoeller-McCormick LM, et al. Dissection of receptor folding and ligand-binding property with functional minireceptors of LDL receptor-related protein. J Cell Sci 2001;114:899–908. [PubMed: 11181173]

Rubin LL, Staddon JM. The cell biology of the blood-brain barrier. Annu Rev Neurosci 1999;22:11–28. [PubMed: 10202530]

Selkoe DJ, Schenk D. Alzheimer's disease: molecular understanding predicts amyloid-based therapeutics. Annu Rev Pharmacol Toxicol 2003;43:545–584. [PubMed: 12415125]

Sharom FJ. The P-glycoprotein efflux pump: how does it transport drugs? J Membr Biol 1997;160:161–175. [PubMed: 9425600]

Shibata M, et al. Clearance of Alzheimer's amyloid-ss(1–40) peptide from brain by LDL receptor-related protein-1 at the blood-brain barrier. J Clin Invest 2000;106:1489–1499. [PubMed: 11120756]

Silverberg GD, et al. Alzheimer's disease, normal-pressure hydrocephalus, and senescent changes in CSF circulatory physiology: a hypothesis. Lancet Neurol 2003;2:506–511. [PubMed: 12878439]

Tanzi RE, et al. Clearance of Alzheimer's Abeta peptide: the many roads to perdition. Neuron 2004;43:605–608. [PubMed: 15339642]

Weiner HL, Frenkel D. Immunology and immunotherapy of Alzheimer's disease. Nat Rev Immunol 2006;6:404–416. [PubMed: 16639431]

Weksler BB, et al. Blood-brain barrier-specific properties of a human adult brain endothelial cell line. Faseb J 2005;19:1872–1874. [PubMed: 16141364]

Zlokovic BV. Clearing amyloid through the blood-brain barrier. J Neurochem 2004;89:807–811. [PubMed: 15140180]

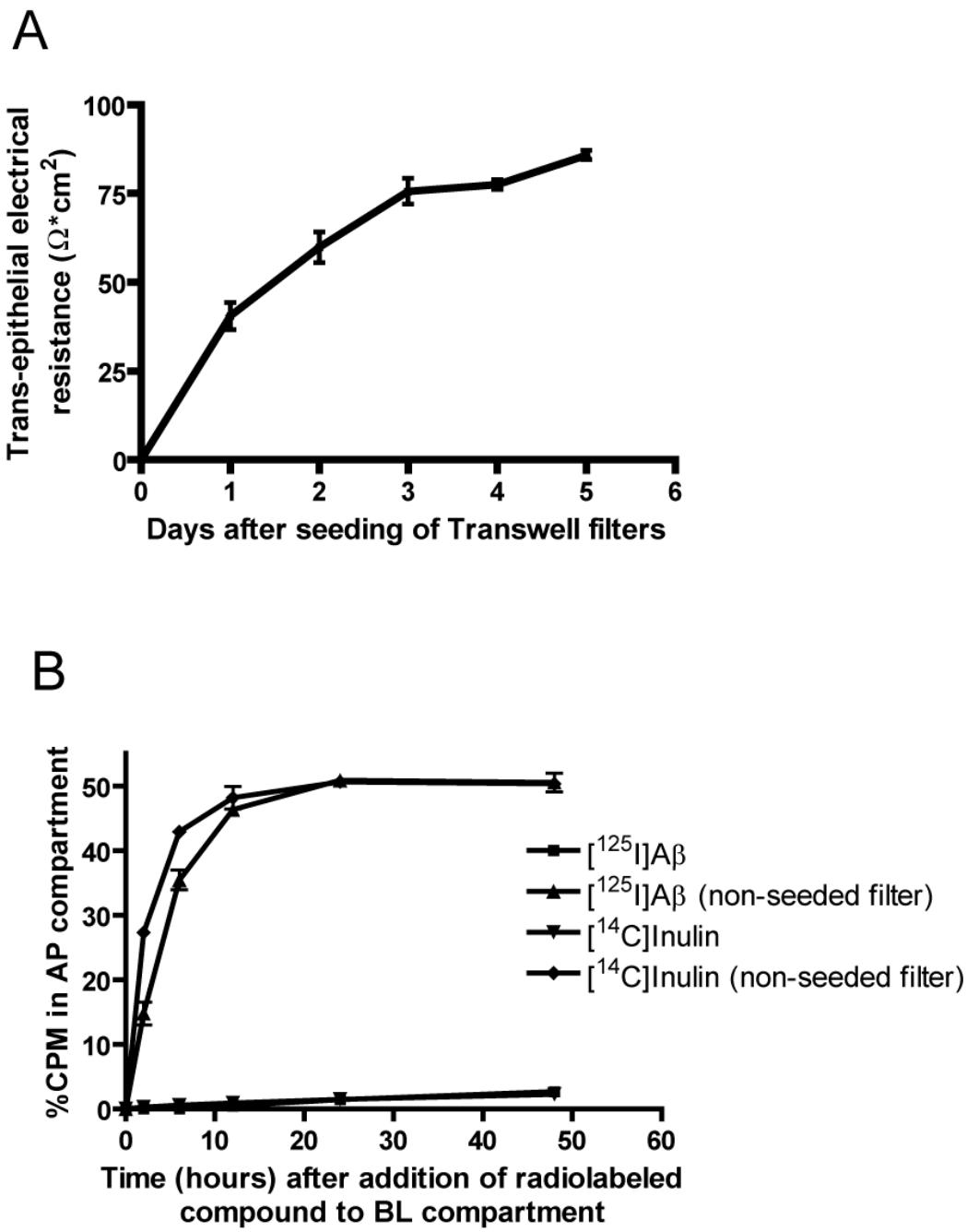

Figure 1.

BBB-like characteristics of the MDCK Transwell model. **A**, Trans-epithelial electrical resistance. TEER increases daily with monolayer growth. Data are mean ± SEM (n=22 independent Transwell filters). **B**, [^{14}C]Inulin and [^{125}I]Aβ permeabilities. Both radiolabeled compounds freely diffuse across non-seeded Transwell filters such that half of the BL-added CPM are found in the AP compartment by 12 hr. In contrast, less than 3% of each molecule is able to cross MDCK monolayers after 48 hr. Data shown are mean ± SD (n=3 at each time point).

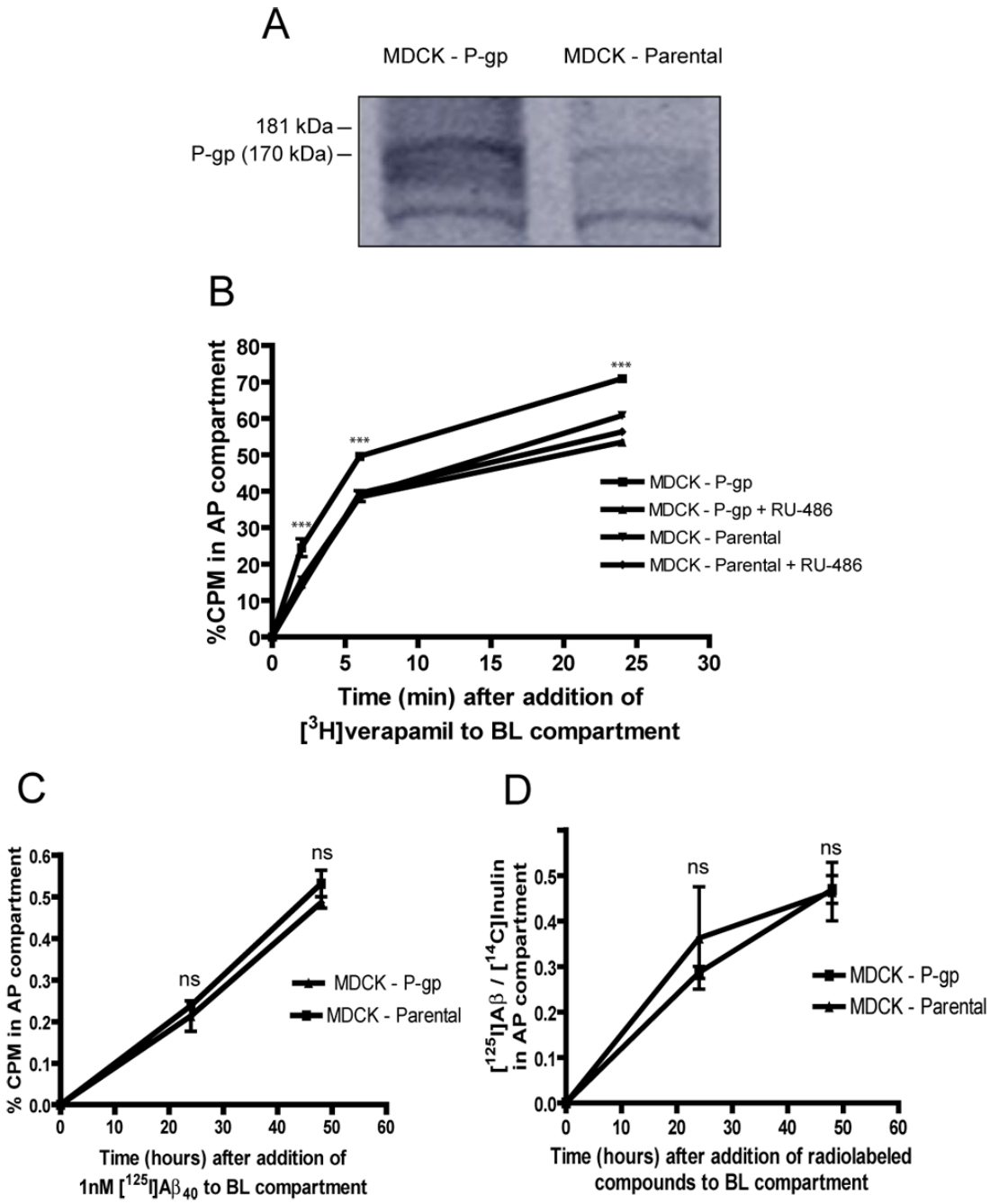

Figure 2.

Pgp upregulation does not promote Aβ transcytosis. **A**, Western blot of Pgp from whole cell lysatses of MDCK-Pgp and MDCK-Parental cells showing increased Pgp expression the former. **B**, Transport of [^{3}H]verapamil across MDCK-Pgp and MDCK-Parental Transwell monolayers. MDCK-Pgp cells express functional Pgp as evidenced by increased BL-to-AP transport of [^{3}H]verapamil across their monolayers compared to that of MDCK-Parental cells ($p<0.001$ at 2, 6 and 24 hr). RU-486, a pharmacological Pgp inhibitor, eliminated this difference when added to MDCK-Pgp monolayers ($p<0.001$ at 2, 6 and 24 hr). **C**, Transport of [^{125}I] Aβ across MDCK-Pgp and MDCK-Parental monolayers MDCK-Pgp monolayers do not exhibit greater BL-to-AP transport of [^{125}I]Aβ than MDCK-Parental monolayers. ($p>0.05$ at

each timepoint). **D**, Aβ clearance quotient, which controls for paracellular leak by dividing Aβ transport by inulin transport, is not significantly different between MDCK-Pgp and MDCK-Parental monolayers ($p>0.05$ at each timepoint). Data shown are mean ± SEM ($n=3$ at each time point).

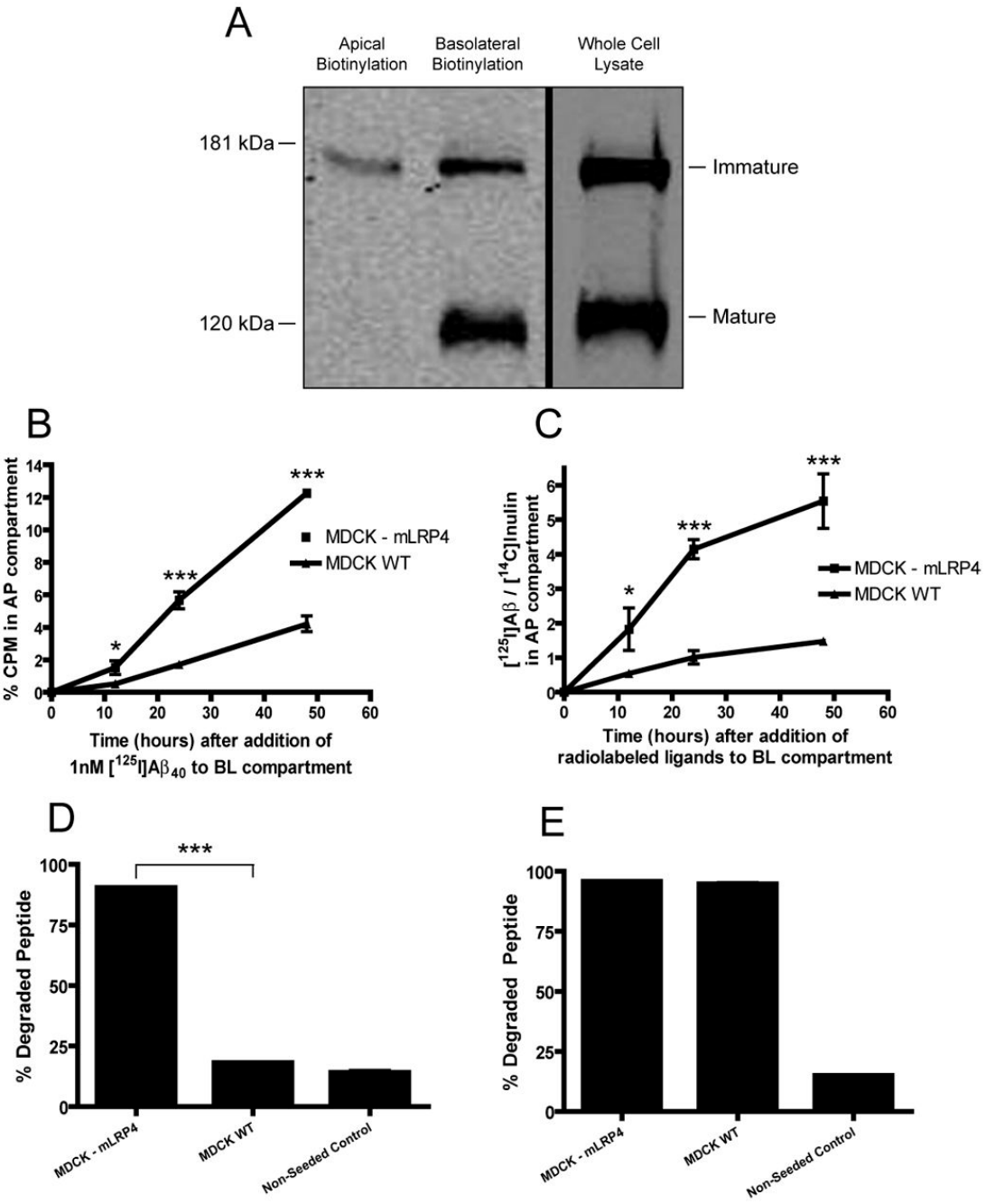

Figure 3.

mLRP4 expression promotes Aβ uptake and intracellular degradation, but not transcytosis. **A**, Western blot of mLRP4 in whole cell lysates, and in apically and basolaterally biotinylated of MDCK-mLRP4 cells on Transwell filters after precipitation with immobilized neutravidin. MDCK-mLRP4 cells express both mature and immature forms of the minireceptor on the BL surface, but only the immature, unprocessed form on the AP surface. **B**, Transport of [^{125}I] Aβ across MDCK-mLRP4 and MDCK wt monolayers. MDCK-mLRP4 monolayers exhibit greater BL-to-AP transport of [^{125}I] counts than MDCK wt monolayers ($p<0.05$ at 12 hr, $p<0.001$ at 24 and 48 hr). **C**, Aβ clearance quotient is significantly higher for MDCK-mLRP4 than for MDCK wt monolayers ($p<0.05$ at 12 hr, $p<0.001$ at 24 and 48 hr). **D**, TCA precipitation

of BL media. MDCK-mLRP4 monolayers degraded significantly more of the [^{125}I]Aβ that was added to the BL compartment than MDCK wt monolayers, accounting for the increased transport of [^{125}I] counts seen in (**B**) and (**C**). **E**, TCA precipitation of AP media. 48 hours after adding 1 nM [^{125}I]Aβ to the BL compartments, nearly all [^{125}I] counts that crossed MDCK-mLRP4 or MDCK wt monolayers were due to degraded peptide fragments. Data shown are mean β SEM (n=3 at each time point). Error bars in **D** and **E** are present, but too small to be seen.

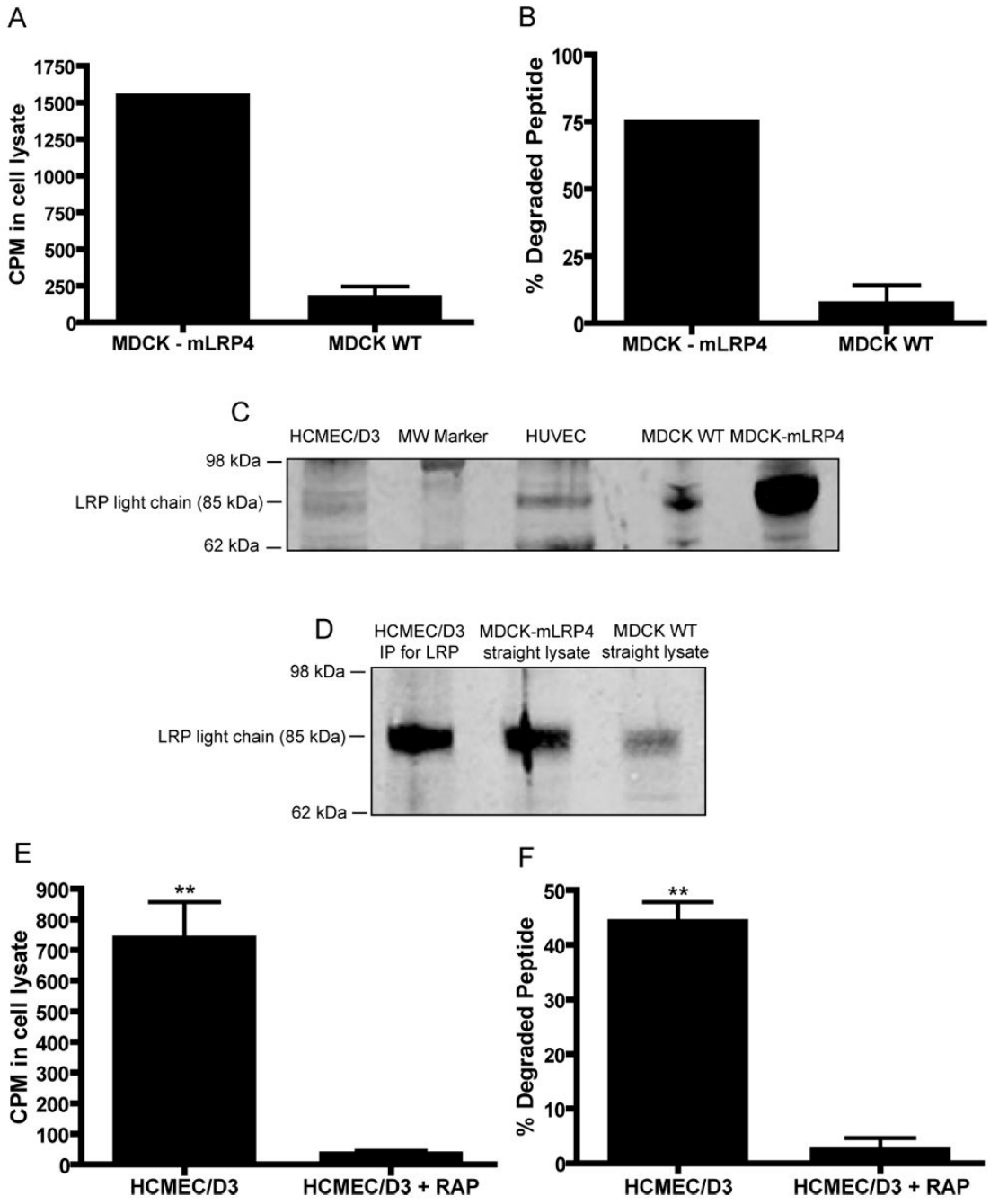

Figure 4.

LRP mediates Aβ endocytosis and intracellular degradation. **A**, [^{125}I] CPM in MDCK-mLRP4 and MDCK wt cell lysates after 24 hr exposure to 1 nM [^{125}I]Aβ. Significantly more [^{125}I] Aβ was endocytosed by MDCK-mLRP4 cells than by MDCK wt cells ($p<0.01$). **B**, TCA precipitation of MDCK-mLRP4 and MDCK wt cell lysates after 24 hr exposure to 1 nM [^{125}I]Aβ. Significantly more intracellular degradation occurred in MDCK-mLRP4 cells than in MDCK wt cells ($p<0.01$). **C**, Western blot of LRP light chain in whole cell lysates (20 μg total protein) of HCMEC/D3, HUVEC, MDCK wt, and MDCK-mLRP4 cells. **D**, Western blot of MMMM-immunoprecipitated LRP light chain from HCMEC/D3 cell lysates (100 μg total protein), and non-precipitated LRP light chain from whole cell lysates (20 μg total protein) of

MDCK-mLRP4 and MDCK wt cells. **E**, [^{125}I] CPM in HCMEC/D3 endothelial cell lysates after 24 hr of exposure to 1 nM [^{125}I]Aβ in the presence or absence of 500 nM RAP. [^{125}I] Aβ endocytosis was significantly inhibited by inhibition of LRP activity by RAP ($p<0.01$). **F**, TCA precipitation of HCMEC/D3 cell lysates after 24 hr exposure to 1 nM [^{125}I]Aβ in the presence or absence of 500nM RAP. [^{125}I]Aβ degradation was significantly inhibited by RAP ($p<0.01$) Data are mean ± SEM (n=3).

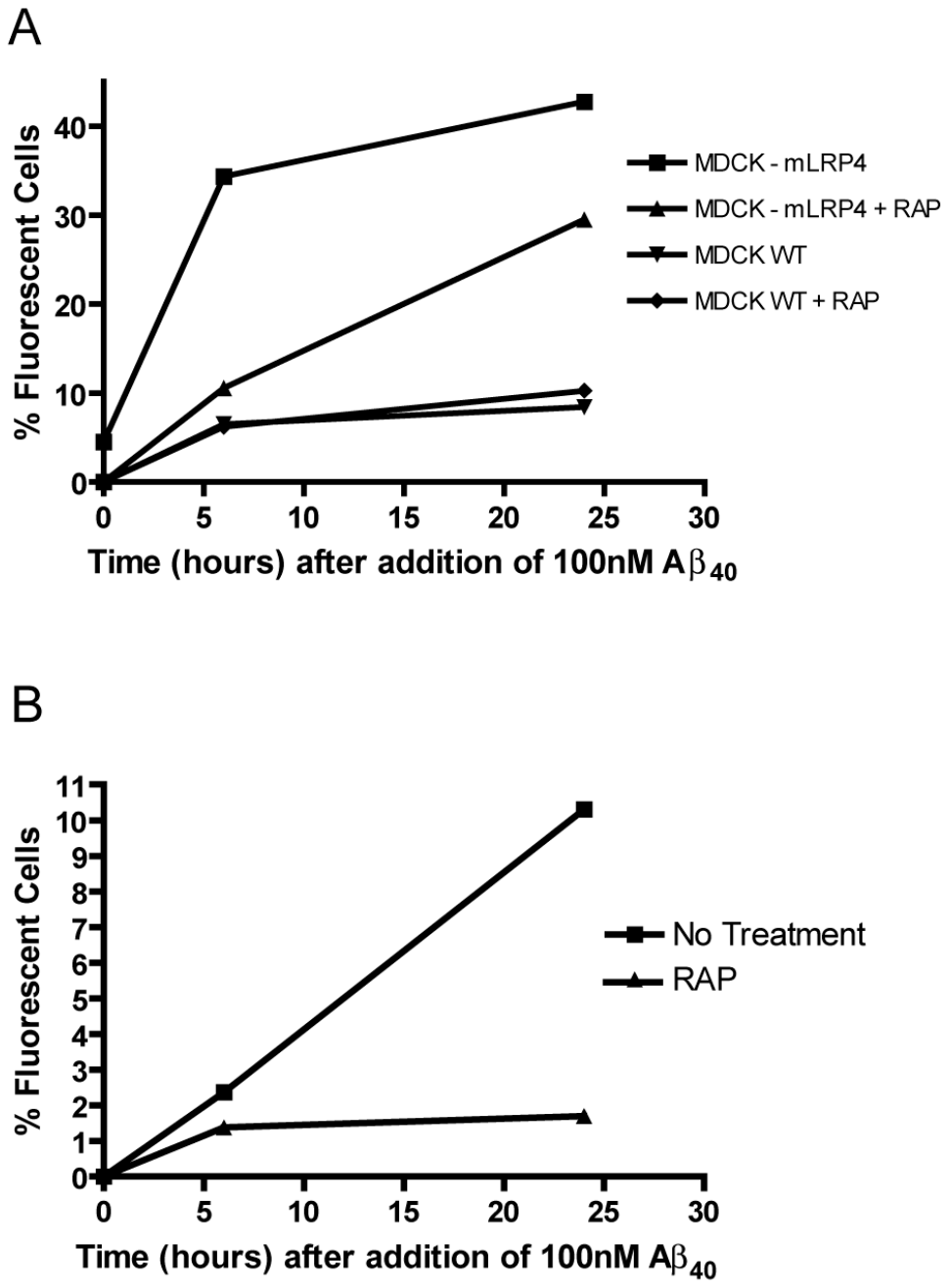

Figure 5.

FACS-based analysis of fluorescently-labeled $A\beta_{40}$ uptake. **A**, MDCK-mLRP4 cells exhibit greater time-dependent uptake of fluorescent Aβ than do MDCK WT cells. This effect of LRP activity was partially reversed by the administering 500 nM RAP. **B**, HCMEC/D3 cells also exhibit time-dependent Aβ uptake that is inhibited by co-administering 500 nM RAP. 1×10^5 cells from each cell population were counted.